Complementary media of electrons

2006 J. Phys.: Condens. Matter 18 3703

(http://iopscience.iop.org/0953-8984/18/15/016)

INSTITUTE OF PHYSICS PUBLISHING JOURNAL OF PHYSICS: CONDENSED MATTER

J. Phys.: Condens. Matter **18** (2006) 3703–3720 doi:10.1088/0953-8984/18/15/016

Complementary media of electrons

Katsuyoshi Kobayashi

Department of Physics, Faculty of Science, Ochanomizu University, 2-1-1 Otsuka, Bunkyo-ku, Tokyo 112-8610, Japan

Received 14 February 2006, in final form 6 March 2006
Published 30 March 2006
Online at stacks.iop.org/JPhysCM/18/3703

Abstract

The concept of complementary media, which cause negative refraction and make perfect lenses, was first introduced to electromagnetic waves. This paper extends it to general waves by expressing the complementarity in terms of a transfer matrix. As an example, complementary media of electrons are discussed theoretically. An application of complementary media to subsurface imaging by scanning tunnelling microscopy is described. For realistic materials the formulation of complementary media is extended to take account of the scattering at interfaces, and effectively complementary systems formed by interfaces are discussed. Interfaces of the graphitic lattice forming complementary systems are designed.

1. Introduction

Pendry and Ramakrishna introduced the concept of complementary media to electromagnetic waves [1]. A complementary medium is a material with permittivity $\varepsilon_c = -\varepsilon$ and permeability $\mu_c = -\mu$, where ε and μ are the permittivity and permeability of an original medium. Electromagnetic fields including evanescent waves have mirror symmetry with respect to the interface plane of original and complementary media. A complete image of an object in an original medium is produced in a complementary medium beyond the diffraction limit of wavelength. Complementary media reproduce the information of amplitude and phase of waves in original media. This property is an origin of negative refraction [2] and perfect lenses [3, 4]. A simple derivation of the complementarity of electromagnetic waves was given by Ruppin [5]. The concept of complementary media has been extended to non-planar geometries [1].

Another viewpoint of complementary media is that a complementary medium completely cancels the evolution of waves in passing through an original medium with an equal thickness. A pair of original and complementary media acts as a space with no thickness, like the pair annihilation of matter and antimatter. This property will be clear when the complementarity is expressed using a transfer matrix. Section 2 presents a formulation of complementary media in terms of a transfer matrix, which is applicable to any wave. Using this formulation we discuss complementary media of electrons in this paper. An application of complementary media is the improvement of resolution in subsurface imaging by scanning tunnelling microscopy.

Ideal examples of application are described in section 3. In realistic materials atomic structures of interfaces are important in the transmission across interfaces. This means that the complementary property is determined not only by the transport properties in media but also by the scattering properties at interfaces. A formulation of complementary media taking account of scattering at interfaces is presented in section 4, which enables us to form effectively complementary systems by tuning the atomic structures of interfaces. Section 5 presents interface structures forming complementary systems designed for the graphitic lattice and demonstrates their complementarity by numerical simulations.

2. Complementary media

Let us start by illustrating the complementarity of electromagnetic waves in terms of a transfer matrix. First we consider homogenous media for simplicity. The Maxwell equations for a monochromatic wave with frequency ω in a medium with permittivity ε and permeability μ are written as

$$\frac{\mathrm{d}E_x}{\mathrm{d}z} = \mathrm{i}\omega\mu H_y \tag{1}$$

$$\frac{\mathrm{d}H_y}{\mathrm{d}z} = \mathrm{i}\omega\varepsilon E_x \tag{2}$$

where we choose x, y and z axes for the directions of electrical field $\mathbf{E}$, magnetic field $\mathbf{H}$ and wave propagation, respectively. These equations are rewritten in a matrix form as

$$\frac{1}{\mathrm{i}}\frac{\mathrm{d}\mathbf{C}}{\mathrm{d}z} = K\mathbf{C} \tag{3}$$

where

$$\mathbf{C} = \begin{pmatrix} E_x \\ H_y \end{pmatrix} \tag{4}$$

and

$$K = \begin{pmatrix} 0 & \omega\mu \\ \omega\varepsilon & 0 \end{pmatrix}. \tag{5}$$

When the fields at $z = z_1$ are given, the fields at $z = z_2$ are obtained from

$$\mathbf{C}(z_2) = T(z_2, z_1)\mathbf{C}(z_1) \tag{6}$$

using a transfer matrix $T(z_2, z_1)$. The transfer matrix for a homogeneous medium is calculated as

$$T(z_2, z_1) = \mathrm{e}^{\mathrm{i}K(z_2 - z_1)}. \tag{7}$$

Since K is transformed to $-K$ under the complementary transformation of $\varepsilon \to -\varepsilon$ and $\mu \to -\mu$, the transfer matrix for the complementary medium is given by

$$T_\mathrm{c}(z_2, z_1) = \mathrm{e}^{-\mathrm{i}K(z_2 - z_1)}. \tag{8}$$

Therefore we obtain a complementary relation of the transfer matrices as

$$T_\mathrm{c}(z_2, z_m)T(z_m, z_1) = 1 \tag{9}$$

when $z_m = (z_1 + z_2)/2$. Complementary media can be defined as media having a transfer matrix which is the inverse of the transfer matrix of the original media. This is satisfied if $K_\mathrm{c} = -K$, where K_c is the matrix of complementary media corresponding to K when the wave equations are written in the form of equation (3).

It can be proved that the complementary relation of the transfer matrices is preserved for electromagnetic fields in inhomogeneous and three-dimensional media as shown in appendix A. Equation (3) has the same form as the time-dependent Schrödinger equation. If we regard the z coordinate as time, complementary media may be considered to be time-reversal materials. The difference from the Schrödinger equation is that K is not necessarily Hermitian, and K may have complex eigenvalues. When the eigenvalues of K are real, waves are propagating. When they are complex, waves are evanescent. The non-Hermitian property enables the amplification of evanescent waves. Matrix K may be regarded as a wavenumber matrix.

It is easy to apply the formalism above to an electronic wavefunction ϕ. We define χ by

$$\chi = \hat{v}\phi = \frac{1}{m}\frac{\hbar}{\mathrm{i}}\frac{\mathrm{d}\phi}{\mathrm{d}z} \tag{10}$$

where $\hat{v}$ is velocity operator. Using a vector defined by

$$\Psi = \begin{pmatrix} \phi \\ \chi \end{pmatrix} \tag{11}$$

the Schrödinger equation is written as

$$\frac{1}{\mathrm{i}}\frac{\mathrm{d}\Psi}{\mathrm{d}z} = K\Psi \tag{12}$$

where

$$K = \begin{pmatrix} 0 & m/\hbar \\ 2(E-V)/\hbar & 0 \end{pmatrix}. \tag{13}$$

In the above E and V are energy and potential. It is obvious that the mass m_c and potential V_c of a complementary medium are given by $m_\mathrm{c} = -m$ and $V_\mathrm{c} = 2E - V$. The conditions for complementary media are the same in the homogeneous three-dimensional case. This can be shown by replacing $E-V$ with $E-V-\hbar^2q^2/(2m)$ in equation (13), where q is the momentum perpendicular to z axis. More generally, when $m_\mathrm{c} = -m$ and $V(x, y, z-z_0)+V_\mathrm{c}(x, y, -z+z_0)$ is constant, it is a complementary medium where $z = z_0$ is the interface of the original and complementary media.

A complementary medium of electrons works at a fixed energy. This is in contrast to the case of electromagnetic waves, where a complementary medium works at any frequency if the permittivity and permeability do not depend on frequency. However, since the permittivity and permeability of real materials are inevitably dispersive and take negative values in limited ranges of frequency, a complementary medium of electromagnetic waves also works in limited ranges of frequency [4]. We may regard a material as a complementary medium when the conditions for complementary media are satisfied at a fixed energy or frequency.

A more general definition of complementary media is given by

$$T_\mathrm{c}(z_\mathrm{c}, 0)T(0, z) = 1 \tag{14}$$

or

$$T_\mathrm{c}(z_\mathrm{c}, 0) = T(z, 0) \tag{15}$$

where we choose the interface plane of the original and complementary media at $z = 0$. z_c is a function of z. If the wavenumber matrix K_c for complementary media is defined by

$$\frac{1}{\mathrm{i}}\frac{\partial T_\mathrm{c}}{\partial z_\mathrm{c}} = K_\mathrm{c}T_\mathrm{c}, \tag{16}$$

we obtain

$$K_\mathrm{c} = \left(\frac{\mathrm{d}z}{\mathrm{d}z_\mathrm{c}}\right)K. \tag{17}$$

When $dz_c/dz = -1$, $K_c = -K$. However, complementary media are not restricted only to this case. Equation (17) expands the class of complementary media. We present such an example in the following.

We consider again a homogeneous medium, but the case with an anisotropic mass as

$$E = \frac{\hbar k^2}{2m_\perp} + \frac{\hbar q^2}{2m_\parallel} + V. \tag{18}$$

In this case the conditions for complementary media are given by

$$\frac{z_c}{z} = -\sqrt{\frac{m_\perp}{m_{c\perp}}\frac{m_{c\parallel}}{m_\parallel}}, \tag{19}$$

$$E = \frac{Vm_\parallel - V_c m_{c\parallel}}{m_\parallel - m_{c\parallel}} \tag{20}$$

and

$$m_\perp m_\parallel = m_{c\perp} m_{c\parallel} \tag{21}$$

with $m_\perp m_{c\perp} < 0$. The first and second conditions are derived from the phase conservation and the last one is from the velocity conservation as shown in appendix B. Here we mean that phase is the product of eigenvalues of matrix K multiplied by position coordinates and velocity is the eigenvalues divided by the (1, 2) element of K.

For isotropic materials, equation (21) is equivalent to $m = -m_c$. But for anisotropic materials the conditions $m_\perp = -m_{c\perp}$ and $m_\parallel = -m_{c\parallel}$ are lifted if the focal distance and energy are chosen as in equations (19) and (20). For example, the case with $m_\perp = -m_{c\parallel}$ and $m_\parallel = -m_{c\perp}$ with $m_\perp m_\parallel < 0$ satisfies the complementary condition. In this case $z_c/z = -|m_\perp/m_\parallel|$. This situation may be realized in anisotropic two-dimensional systems if two identical anisotropic materials are jointed on a line with rotated by 90° each other.

The discussion presented above is a simple one, in which we implicitly assumed that the fields conveyed by a transfer matrix are continuous across the interfaces of the original and complementary media. In discussing complementary media of realistic materials it is necessary to generalize the definition of the complementary media with taking account of the scattering caused by the atomic structures of the interfaces. This will be presented in section 4. Before the discussion on the connection of fields at interfaces we present an application of complementary media to subsurface imaging in the next section.

3. Subsurface imaging using complementary media

An application of complementary media is the improvement of subsurface imaging by scanning tunnelling microscopy (STM). STM is a method for studying topography and electronic states of solid surfaces on atomic scales. The information obtained by STM is usually that of the outermost layers of surfaces. However, there are some experimental images showing information of subsurface structures. For example, long-period structures like moiré patterns appear in the images of layered materials [6] and the images of bulk impurities buried in semiconductor surfaces are observed [7–11]. A theory on the mechanism of observation of subsurface structures in STM has been presented [12], in which it is essential that the short-wavelength waves on atomic scales parallel to surfaces are evanescent waves in materials and the long-wavelength waves on nanometre scales are propagating ones. The former waves of the outermost layers are observed in STM as atomic-scale corrugation and the latter ones produced by subsurface irregularities appear as long-wavelength structures. According to this theory the resolution of the images of subsurface structures is limited by the wavelengths of propagating

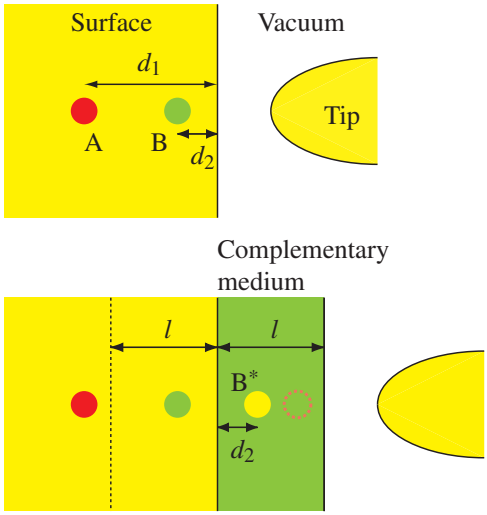

Figure 1. Schematic diagram of subsurface imaging using complementary media. Impurity A buried at depth d_1 and hindered by obstacle B is seen at depth $d_1 - l$ indicated by the dotted circle when a complementary medium with thickness l with an anti-obstacle B* is laid on the surface.

(This figure is in colour only in the electronic version)

waves and the amplitude of subsurface images decreases accompanied with oscillation as the depth of the subsurface structures increases. However, it may be possible to improve the resolution by using complementary media. We present two ideal examples below.

The first example is a simple one. We consider impurity A buried at depth d_1 in a surface. When a complementary medium with thickness l is laid on the surface, the image of the impurity is seen as if it is buried at shallower depth $d_1 - l$.

The second example is the case that impurity A is hindered to be seen behind obstacle B buried at depth d_2, as shown schematically in figure 1. In this case interference between A and B may provide information about impurity A without a complementary medium. But the pure image of impurity A is directly observed at depth $d_1 - l$ if the complementary medium with thickness l is laid on the surface and anti-obstacle B* is buried in the complementary medium symmetrically with respect to the interface of the original and complementary media.

In order to demonstrate some feasibility of these ideas we simulate the images of subsurface impurities with and without complementary media using realistic material parameters. Figure 2 shows simulated images of subsurface impurities corresponding to the two examples. The method of calculations is the same as that in [13]. We use a screened Coulomb potential

$$V(r) = f_0 \frac{\mathrm{e}^{-\mu r}}{r} \tag{22}$$

for the impurity potential. We choose 0.066 and 0.0529 au for f_0 and μ, respectively, where au is atomic units ($m_e = \hbar = e = 1$). We assume that the potential in the surface is constant. The potential and Fermi energies are $-0.150\,5445$ and -0.15 au measured from the vacuum level, respectively. These parameters are chosen to reproduce the STM images of Si impurities in GaAs(110) surfaces [10]. Details of the choice of parameters are given in [13]. STM images are simulated using the local density of states of surfaces at a tip [14]. The height of the images is expressed in the logarithmic scale as $\ln[\rho(r_\parallel)/\rho(\infty)]$, where $\rho(r_\parallel)$ is the local density of states at distance $r_\parallel$ from the centre of the images of impurities. The images are simulated in the

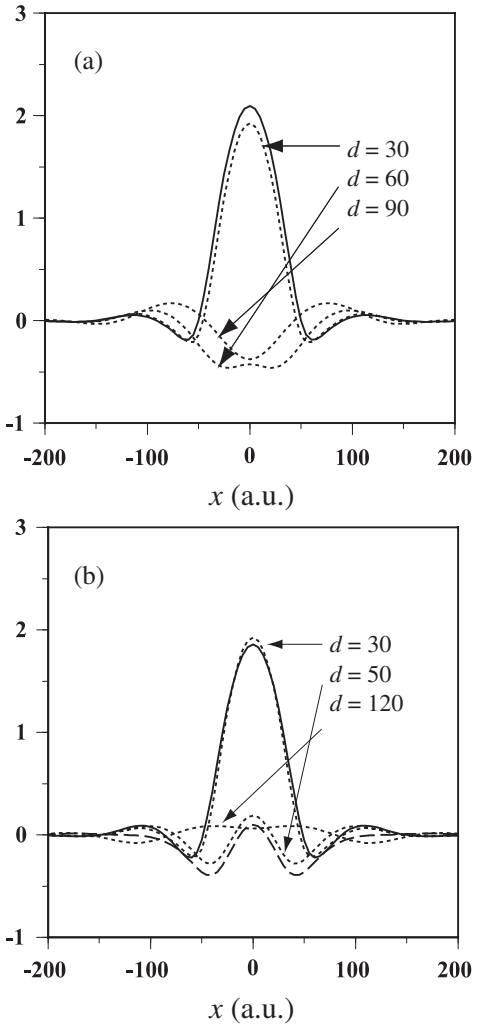

Figure 2. Simulated images of subsurface impurities. The horizontal axis shows the coordinates parallel to the surface. The vertical axis shows the logarithm of local density of states normalized by that at a distance of 200 au from the centres of the images of impurities. The dotted lines show the images of single impurities buried at depth d (au). (a) The solid line shows the image of a single impurity buried at a depth of 60 au when the surface is covered with a complementary slab with a thickness of 30 au. (b) The broken line shows the image of double impurities buried at depths of 50 and 120 au. The solid line shows the image of double impurities buried at depths of 50 and 120 au when the surface is covered with a complementary slab with a thickness of 90 au and an anti-impurity corresponding to the impurity at 50 au is buried in the complementary slab.

constant-height mode. The local density of states is calculated on a plane in the vacuum region 10 au distant from the surface. $\rho(\infty)$ is approximated by the value at a position sufficiently distant from the centre of the impurity images.

Figure 2(a) shows images of single impurities. The dotted lines show the images of impurities without a complementary medium. The amplitude of the images decreases with increasing the depth of impurities. The origin of the oscillation in the images is the interference of the standing waves formed by the vacuum barrier and the scattered waves by impurities [13].

The solid line shows an image of an impurity buried at a depth of 60 au in a surface which is covered with a complementary medium with a thickness of 30 au. The impurity is buried at a depth of 90 au in total from the top of the complementary medium, but the image is almost the same as that of the impurity at a depth of 30 au without a complementary medium. The incompleteness in reproduction is ascribed to numerical inaccuracy.

Figure 2(b) shows the images of impurities corresponding to the case in figure 1. The dotted lines show the images of single impurities without a complementary medium. The amplitude of the image of the impurity at a depth of 120 au is very small. The image of double impurities at depths of 50 and 120 au shown by the broken line is similar to the image of a single impurity at a depth of 50 au, and it is hard to obtain any information about the impurity at 120 au. However, when a complementary medium with a thickness of 90 au is laid on the surface and an anti-impurity corresponding to the impurity at 50 au is buried in the complementary medium symmetrically with respect to the interface of the surface and the complementary medium, the image of the impurity at 120 au is distinctly visible as if it is buried at a depth of 30 au from the top of the complementary medium, as shown by the solid line.

These examples require ideal situations and may be difficult to be realized in the strict way. But it may be possible to improve the resolution of subsurface imaging by making use of complementary media.

4. Complementary systems of realistic materials

The wavelength of an electron in materials is as short as atomic distances. This is true even in semiconductors, where the wavelength of envelope functions is usually much longer than atomic scales. The connection condition of wavefunctions of two media depends on the atomic structures of the interface. In this point electrons are different from electromagnetic waves with wavelength of light or microwaves and on the one hand this makes it difficult to realize complementary media of electrons. However, on the other hand this produces the possibility of realizing effectively complementary systems by tuning the interface structures. An example is presented in the next section. This section presents a formal discussion.

The connection of wavefunctions of, for example, one-dimensional systems is determined by two conditions. For bare wavefunctions the wavefunction and the first derivative are continuous across an interface. The connection conditions of envelope functions at an interface of two semiconductors A and B are expressed by a 2×2 matrix T_I [15, 16] given by

$$\begin{pmatrix} \phi_{\mathrm{B}}(0) \\ \chi_{\mathrm{B}}(0) \end{pmatrix} = T_I \begin{pmatrix} \phi_{\mathrm{A}}(0) \\ \chi_{\mathrm{A}}(0) \end{pmatrix} \tag{23}$$

where $\phi_i(x)$ and $\chi_i(x)$ are a wavefunction of semiconductor i and a function multiplied by the velocity operator defined in equation (10), respectively. The position of the interface is $x = 0$. The current conservation across interfaces leads to a relation

$$T_I^{\dagger} \begin{pmatrix} 0 & 1 \\ 1 & 0 \end{pmatrix} T_I = \begin{pmatrix} 0 & 1 \\ 1 & 0 \end{pmatrix}. \tag{24}$$

This does not necessarily mean that T_I is a unit matrix.

The interface matrix has been calculated for various types of semiconductor heterointerfaces using a tight-binding model and an empirical pseudopotential model [16]. The calculation shows that the current conservation holds fairly well. The form of the interface matrix depends on the type of connection of energy bands. The interface matrix is diagonal in the cases of connecting conduction bands and connecting light-hole valence bands at the $\mathrm{GaAs/Al}_x\mathrm{Ga}_{1-x}\mathrm{As}$ interface. The diagonal elements of the interface matrix are zero in the case

of connecting the valence and conduction bands at the GaSb/InAs interface. In this case the envelope function and the first derivative are interchanged at the interface.

It is theoretically predicted that negative refraction of ballistic electrons may occur at twin boundaries of uniaxial semiconductors [17]. In this theory the continuity of wavefunctions and current is assumed in connecting envelope functions at interfaces, which corresponds to the interface matrix being unity. The negative refraction at twin boundaries has an advantage that the refraction is always reflectionless at any energy. But it is not a complementary system because both positive and negative refraction take place at fixed energy depending on the angle of incidence.

When the interface matrix T_I is not unity or more generally non-commutative with the transfer matrix, the condition for complementary media in equation (14) is modified to

$$T_{\rm c}(z_{\rm c},0)T_I T(0,z) = T_I. \tag{25}$$

The right-hand side of the equation is not unity, because the left-hand side is T_I for $z = 0$. The complementarity condition on wavenumber matrix $K_{\rm c}$ in equation (17) is also modified to

$$K_{\rm c} = \left(\frac{{\rm d}z}{{\rm d}z_{\rm c}}\right) T_I K T_I^{-1}. \tag{26}$$

A simple example is that $K_{\rm c} = K$ when

$$T_I = \begin{pmatrix} 1 & 0 \\ 0 & -1 \end{pmatrix}, \tag{27}$$

${\rm d}z/{\rm d}z_{\rm c} = -1$ and K is given by equation (13). This result means that a complementary system can be formed only by tuning the transmission properties through an interface.

When the interface matrix has a form of

$$T_I = \begin{pmatrix} 0 & a \\ 1/a^* & 0 \end{pmatrix} \tag{28}$$

and K given by equation (13) is written as

$$K = \begin{pmatrix} 0 & p \\ q & 0 \end{pmatrix}, \tag{29}$$

$K_{\rm c}$ is calculated as

$$K_{\rm c} = \frac{{\rm d}z}{{\rm d}z_{\rm c}} \begin{pmatrix} 0 & q|a|^2 \\ p/|a|^2 & 0 \end{pmatrix}. \tag{30}$$

The phase conservation, i.e. the conservation of eigenvalues of K multiplied by position coordinates, is

$$p_{\rm c}q_{\rm c} = \left(\frac{{\rm d}z}{{\rm d}z_{\rm c}}\right)^2 pq \tag{31}$$

which is the same as the case that T_I is unity. But the velocity conservation is

$$|a|^4 v^2 v_{\rm c}^2 = 1 \tag{32}$$

where $v^2 = q/p$ and $v_{\rm c}^2 = q_{\rm c}/p_{\rm c}$. This equation has solutions of

$$E = \frac{V + V_{\rm c}}{2} \pm \sqrt{\left(\frac{V - V_{\rm c}}{2}\right)^2 + \frac{mm_{\rm c}}{4|a|^4}}. \tag{33}$$

The conditions of complementary systems are satisfied only when

$$mm_{\rm c} > -|a|^4 (V - V_{\rm c})^2. \tag{34}$$

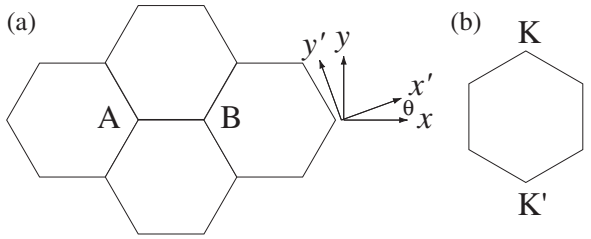

Figure 3. Atomic structure (a) and Brillouin zone (b) of two-dimensional graphite.

In the multi-dimensional cases there is no solution satisfying the conditions of complementary systems for arbitrary wavevector parallel to the interface. However, this conclusion is applied only to electron bands with quadratic dispersions. When the electron bands have non-quadratic dispersions, different conclusions may be drawn. An example is found in the two-dimensional graphitic lattice, where electron bands have massless dispersions. We present the interfaces forming complementary systems of the graphitic lattice in the next section.

5. Complementary systems of the graphitic lattice

We consider transmission through interfaces of graphitic lattices. Figure 3 shows the atomic structure and Brillouin zone of two-dimensional graphite. A unit cell of two-dimensional graphite contains two kinds of carbon atom, labelled A and B. The electronic states near the Fermi energy are expressed by a linear combination of π orbitals of carbon atoms. The two π bands touch at two points, labelled K and K′ in the Brillouin zone, which are the positions of the Fermi energy [18]. The energy dispersions nearby points K and K′ are approximately linear like light, and have an electron–hole symmetry. Due to the massless dispersions the discussions for free electrons in sections 2 and 4 are not applicable. We seek complementary systems of the graphitic lattice in the following way.

First we consider the effective-mass equation of the graphitic lattice [19, 20] given by

$$\begin{pmatrix} 0 & \gamma(-\mathrm{i}\hat{k}_x+\hat{k}_y) & 0 & 0 \\ \gamma(\mathrm{i}\hat{k}_x+\hat{k}_y) & 0 & 0 & 0 \\ 0 & 0 & 0 & \gamma(-\mathrm{i}\hat{k}_x-\hat{k}_y) \\ 0 & 0 & \gamma(\mathrm{i}\hat{k}_x-\hat{k}_y) & 0 \end{pmatrix} \begin{pmatrix} F_{\mathrm{A}}^{\mathrm{K}} \\ F_{\mathrm{B}}^{\mathrm{K}} \\ F_{\mathrm{A}}^{\mathrm{K}'} \\ F_{\mathrm{B}}^{\mathrm{K}'} \end{pmatrix} = E \begin{pmatrix} F_{\mathrm{A}}^{\mathrm{K}} \\ F_{\mathrm{B}}^{\mathrm{K}} \\ F_{\mathrm{A}}^{\mathrm{K}'} \\ F_{\mathrm{B}}^{\mathrm{K}'} \end{pmatrix} \tag{35}$$

where $\gamma = (\sqrt{3}/2)at_{\mathrm{pp}\pi}$, $\hat{k}_x = \frac{1}{\mathrm{i}}\frac{\partial}{\partial x}$ and $\hat{k}_y = \frac{1}{\mathrm{i}}\frac{\partial}{\partial y}$. a and $t_{\mathrm{pp}\pi}$ are the lattice constant of graphite and the transfer energy between π orbitals. $F_{\mathrm{A}}^{\mathrm{K}}$ is an envelope function of the A sublattice expressing a state near point K, and so on. The origin of energy is that of points K and K′. The effective-mass approximation is valid only for waves with wavelengths much longer than the lattice constant.

When we assume a plane wave with wavenumber k_y for the y direction, the effective-mass equation is written as

$$\frac{\mathrm{d}}{\mathrm{d}x} \begin{pmatrix} F_{\mathrm{A}}^{\mathrm{K}} \\ F_{\mathrm{B}}^{\mathrm{K}} \\ F_{\mathrm{A}}^{\mathrm{K}'} \\ F_{\mathrm{B}}^{\mathrm{K}'} \end{pmatrix} = \begin{pmatrix} -k_y & E/\gamma & 0 & 0 \\ -E/\gamma & k_y & 0 & 0 \\ 0 & 0 & k_y & E/\gamma \\ 0 & 0 & -E/\gamma & -k_y \end{pmatrix} \begin{pmatrix} F_{\mathrm{A}}^{\mathrm{K}} \\ F_{\mathrm{B}}^{\mathrm{K}} \\ F_{\mathrm{A}}^{\mathrm{K}'} \\ F_{\mathrm{B}}^{\mathrm{K}'} \end{pmatrix}. \tag{36}$$

It is clear that if there is an interface interchanging the A and B sublattices of graphite but keeping the waves at K and K′, it is an interface forming a complementary system.

When we assume a plane wave with wavenumber k_x for the x direction, the effective-mass equation is written as

$$\frac{1}{\mathrm{i}}\frac{\mathrm{d}}{\mathrm{d}y}\begin{pmatrix} F_{\mathrm{A}}^{\mathrm{K}} \\ F_{\mathrm{B}}^{\mathrm{K}} \\ F_{\mathrm{A}}^{\mathrm{K}'} \\ F_{\mathrm{B}}^{\mathrm{K}'} \end{pmatrix} = \begin{pmatrix} -\mathrm{i}k_x & E/\gamma & 0 & 0 \\ E/\gamma & \mathrm{i}k_x & 0 & 0 \\ 0 & 0 & \mathrm{i}k_x & -E/\gamma \\ 0 & 0 & -E/\gamma & -\mathrm{i}k_x \end{pmatrix} \begin{pmatrix} F_{\mathrm{A}}^{\mathrm{K}} \\ F_{\mathrm{B}}^{\mathrm{K}} \\ F_{\mathrm{A}}^{\mathrm{K}'} \\ F_{\mathrm{B}}^{\mathrm{K}'} \end{pmatrix}. \tag{37}$$

Therefore if there is an interface that interchanges the waves at K and K′, keeping the A and B sublattices, it produces a complementary system. It is possible to prove that there are only these two cases that form complementary systems, as shown in appendix C.

We design the atomic structures of interfaces corresponding to these two cases by inserting one-dimensional structures consisting of polygons into the hexagonal graphitic lattice. In designing, we consider only the interface structures consisting of only even-member rings in order to maintain the electron–hole symmetry. The tight-binding equations of the graphitic lattice with nearest-neighbour interaction are given by

$$Ea_i = -t_{\mathrm{pp}\pi}\sum_j b_j \tag{38}$$

and

$$Eb_i = -t_{\mathrm{pp}\pi}\sum_j a_j \tag{39}$$

where a_i and b_j are coefficients of the atomic orbitals at the ith and jth sites of sublattices A and B, respectively. The summation is taken over three nearest-neighbour atoms. In the above we neglect the overlap integral between π orbitals. The electron–hole symmetry is evident from the transformation of $a_i \to a_i$ and $b_i \to -b_i$. Therefore, to preserve the electron–hole symmetry, the A and B sublattices should be well-defined, which means that odd-member rings are unacceptable to interface structures.

The reason for keeping the electron–hole symmetry is as follows. The Fermi surfaces of the two-dimensional graphite are points at K and K′ and most of the states are evanescent waves near the Fermi energy. Therefore interface-state bands must exist to form a complementary system. If an interface-state band exists and has a point with energy $E = 0$ in the Brillouin zone, it should be a dispersionless band at $E = 0$ in two-channel systems due to the electron–hole symmetry. The other channel is an anti-interface state. Here we mean by anti-interface state such a state that the wavefunction increases exponentially on both sides of an interface with increasing the distance from the interface. These properties are conditions favourable for complementary systems. Therefore it is also desirable that there are only two channels in the systems. This means that the unit cell of the direction parallel to the interfaces should be the same size as that of the graphitic lattice.

Figure 4 shows two examples of atomic structures satisfying the requirements above. One is an interface of zigzag edges of graphitic lattices and the other is an interface of armchair edges, where the terms of zigzag and armchair edges are as used in defining the types of carbon nanotube [21]. The interfaces consist of sites having only two π bonds. Here we do not discuss how the sites with two π bonds are realized but proceed to calculations of the electronic states and transport properties of these interfaces. Some suggestions on realistic structures will be presented at the end of this section.

These interfaces change all decaying waves to growing waves and vice versa at energy $E = 0$ in the full range of the Brillouin zone. The details of the tight-binding calculations are given in appendices D and E. One deviation from perfect complementary systems is the difference by π between the phases of the A and B sublattices after passing through the

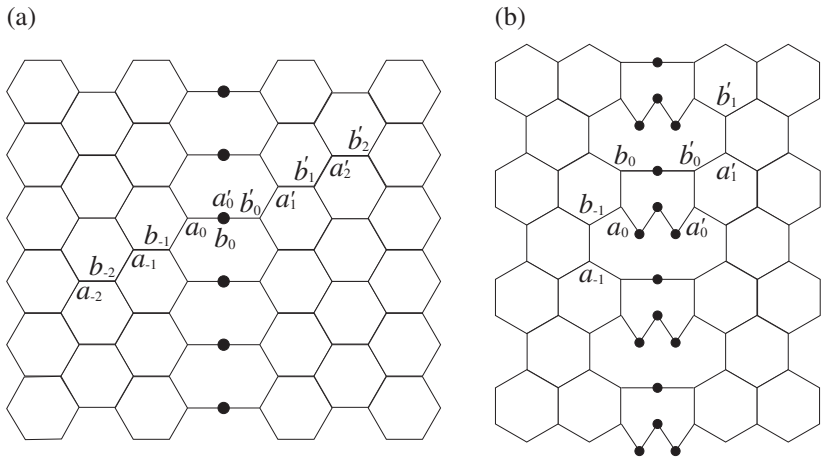

Figure 4. Interface structures forming complementary systems of the graphitic lattice. Closed circles show sites with only two π bonds.

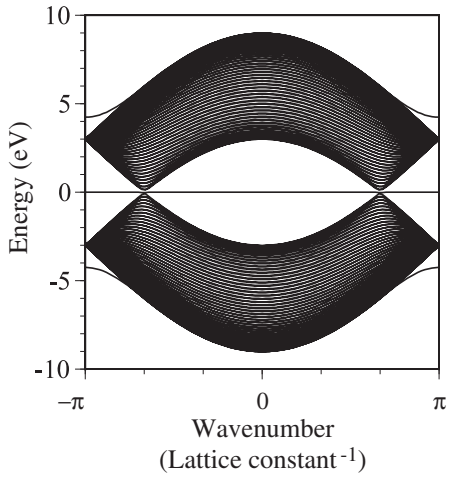

Figure 5. Band structure of the interface in figure 4(a) calculated using a supercell.

interfaces. However, the difference in phase is compensated after passing through double interfaces. Therefore these interfaces work as structures forming complementary systems.

Figure 5 shows a band structure of the interface in figure 4(a). The band structure is calculated using a supercell in the direction perpendicular to the interface. The supercell consists of 100 unit cells of the graphitic lattice and one interface atom. We choose 3.0 eV for $t_{pp\pi}$, because experimental and theoretical values range from 2.6 to 3.2 eV [22].

The regions filled with many lines are the continuum bands of two-dimensional graphite. Outside of the continuum two kinds of interface state exist. One is a flat band at $E = 0$ and the other is dispersive bands around ± 4 eV. It is known that a Shockley-type surface state exists at the zigzag edge of a graphitic lattice [23–25]. However, the surface state of the graphite edge exists in only a restricted region of the Brillouin zone. The present interface state exists in the full range of the Brillouin zone, which is a property necessary for forming a complementary system.

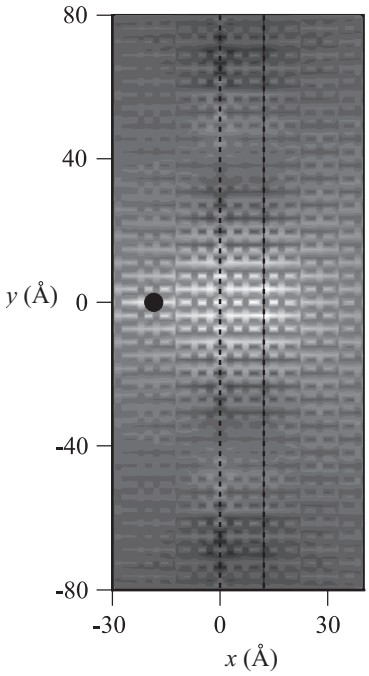

Figure 6. Current distribution in the graphitic lattice with double interfaces. Each interface structure is that in figure 4(a). The dotted lines and closed circle show the positions of the interface lines and the impurity site, respectively. The energy of scattering states is −0.1 eV. Current flows from left to right.

In order to show directly the complementary property of the interface we calculate the transmission across the interface. We consider a double-interface system in which a graphitic lattice is separated into three regions (I, II, III) by double interfaces. Each interface structure is that in figure 4(a). The distance between the centre lines of the two interfaces is 12.07 Å, which corresponds to five unit cells of the graphitic lattice inserted between the two interfaces. All the transfer energies between nearest-neighbour sites are the same. The onsite energy at only one site in region I is shifted by +1.0 eV. We regard this site as an impurity. The distance between the impurity site and the interface nearer to the impurity is 18.46 Å, which corresponds to the site in the ninth unit cell of the graphitic lattice numbered from the interface.

We solve the wavefunctions of scattering states and calculate the current distribution. The method of calculations is the same as that in [26]. We impose a periodic boundary condition on the direction parallel to the interface lines. The size of the supercell is 305 unit cells of the graphitic lattice, which corresponds to 750 Å in length. The current distribution is calculated using only the states in which the Bloch wavenumber of the supercell parallel to the interface lines is zero.

Figure 6 shows the current distribution. Current is incident on the double interface from the side including the impurity site. The figure shows the distribution of the amount of currents flowing to the nearest-neighbour sites in front of each site. The energy of the scattering states is −0.1 eV measured from the Fermi energy of two-dimensional graphite. Though the unit length in the y direction is 750 Å, only the region near the impurity is shown. The current is large near the interfaces and in front of the impurity, which reflects the wavefunctions of the interface states. The current distribution is approximately symmetrical with respect to both the interface lines, which evidences the complementarity of the system.

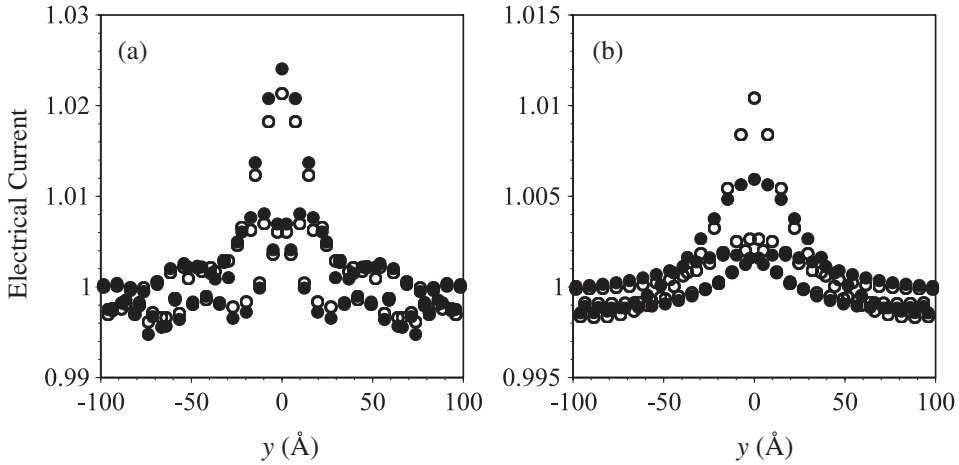

Figure 7. Images of impurities in graphitic lattices with (a) and without (b) double interfaces forming a complementary system. Closed and open circles in (a) show the currents on lines $x = 14.20$ and -9.94 Å in figure 6, respectively. Those circles in (b) are on lines $x = 12.78$ and $x = -9.94$ Å. Current is normalized by the average value over the y direction.

In order to confirm the complementary property more directly, images of the impurity are shown in figure 7. The images are expressed by the currents on lines $x = -9.94$ and 14.20 Å in figure 6. The symmetrical line of $x = -9.94$ with respect to the interface on $x = 0$ is $x = 9.94$, which is also the symmetrical line of $x = 14.20$ with respect to the other interface on $x = 12.07$. Therefore it is expected that the original image on $x = -9.94$ is reproduced by the image on $x = 14.20$. For comparison, the images of the impurity in a perfect graphitic lattice without the double interfaces are calculated and shown in figure 7(b). Since there is no atom on line $x = 14.20$ in this structure, the image on line $x = 12.78$ which is nearer to the impurity than $x = 14.20$ is shown instead. Though the image, for example, shown by closed circles in figure 7(b) may look like a superposition of three images, it is a single image consisting mainly of three components of waves.

The numerical result shows that the image after passing through the complementary region almost reproduces the original image. We define corrugation by the maximum deviation from the average value. In the case without the complementary region, the corrugation decreases monotonically with the distance from the impurity. The corrugation amplitude on $x = -9.94$ is reduced to that on $x = 12.78$ by a factor of 0.57. However, in the case with the complementary region, the corrugation amplitudes on lines $x = -9.94$ and $x = 14.20$ are not much different. On the contrary, it slightly increases by a factor of 1.13. The width of the impurity image broadens without the complementary region as the distance from the impurity increases. But the resolution of the impurity image with the complementary region does not much differ on lines $x = -9.94$ and 14.20. The imperfection in reproduction originates from the slight deviation in energy from zero, which is the only energy where the complementary condition is strictly satisfied. We verified numerically that the reproducibility is improved as the energy approaches zero. The numerical result shows that the complementary property is fairly good, even for energy different by about 0.1 eV from that of the strict complementary condition.

The wavelength of propagating waves expressed by the envelope function is about 400 Å at the energy of -0.1 eV. The widths of the images are narrower than this wavelength. Therefore all the images in figure 7 consist of evanescent waves, which was confirmed by analysing the

components of the wavefunctions. Since the wavelengths of the evanescent waves forming the images are relatively long in the direction parallel to the surface, the decay of the evanescent waves is relatively slow in the perpendicular direction.

We have not discussed the stability and the way of realization of the interface structures presented in this section. The sites with two π bonds may be realized by attaching hydrogen atoms to the carbon atoms constituting the interfaces. It is expected that the structure in figure 4(b) is more difficult to be realized than that in figure 4(a) because of the jammed structure. However, the tight structure may be loosened by adding chains into the interface atoms. It can be shown that complementary systems are formed when all the chains of two-bond sites connecting the two graphitic structures in the interface structures of figure 4 are simultaneously lengthened with identical even numbers of two-bond sites.

In any case, real atomic structures are accompanied by reconstructions, and it would be difficult to fabricate complementary systems in the strict sense. But as demonstrated in the numerical calculations, the complementary property emerges even if the conditions for complementary systems are not strictly satisfied. It may be realized to improve the resolution of subsurface images by devising atomic structures of interfaces.

6. Conclusion

In this paper we have described the complementary media of electrons. First we presented a formulation of complementary media in terms of a transfer matrix. We presented a definition of complementary media that the transfer matrix of complementary media is the inverse matrix of the transfer matrix of original media. This definition is applicable to any wave. We expressed the condition of complementary media in terms of a wavenumber matrix, where the space-reversal property of complementary media including evanescent waves is clear. Using the expression in terms of the wavenumber matrix we obtained the conditions of complementary media for free electrons. The definition of complementary media was generalized to the cases without mirror symmetry, and we discussed the conditions of complementary media for electrons with anisotropic effective mass, which are derived from the phase and velocity conservations.

Second, we described an application of complementary media to subsurface imaging in scanning tunnelling microscopy. We showed the possibility of imaging subsurface structures beyond the wavelength limit of electrons by making use of complementary media. We presented two ideal examples of imaging subsurface impurities. One is a simple subsurface impurity and the other is an impurity hindered from imaging by an obstacle. We simulated the impurity images for both cases and demonstrated the possibility of improving the resolution of subsurface imaging by using complementary media.

The formulation of complementary media was extended to take account of the scattering at interfaces. The reason for this extension is that the wavelength of electrons in materials is the same order as the atomic distances, and the atomic structures of interfaces are important in determining the transmission properties across interfaces. The extended formulation makes it possible to form effectively complementary systems only by tuning transmission properties at interfaces.

Finally, we discussed the complementary media of the graphitic lattice and designed the interface structures forming complementary systems. A discussion using an effective-mass equation suggested two types of interface that form complementary systems. One is the interfaces that interchange the A and B sublattices of the graphitic lattice while keeping the waves at points K and K$'$ in the Brillouin zone. The other is those having reverse properties. We designed the atomic structures of the interfaces corresponding to these cases and proved

the complementarity of the interfaces at the Fermi energy using a tight-binding model. The interfaces have interface states without dispersion at the Fermi energy in the full range of the Brillouin zone, which is a condition necessary for forming complementary systems. We simulated the images of an impurity in the graphitic lattice with and without a complementary region formed with double interfaces, and verified that the interfaces work well as structures showing complementary properties even when the complementary conditions are not strictly satisfied.

This paper has presented only theoretically the possibility of complementary media or systems of electrons. Their realization is left as a difficult problem to be solved in future. Of course, this paper does not enumerate all the cases and applications of complementary media and systems. It is quite probable that different types of complementary media and interfaces forming complementary systems will be found. This paper may provide a clue to finding and designing new complementary media and interface structures.

Acknowledgment

Numerical calculations were performed using supercomputers at the Institute of Solid State Physics, University of Tokyo.

Appendix A

This appendix presents the complementary property of electromagnetic fields in three dimensions. We define a vector as

$$\mathbf{F} = {}^{t}(E_x, E_y, H_x, H_y). \tag{A.1}$$

The Maxwell equations for frequency ω lead to an equation as

$$\frac{1}{\mathrm{i}}\frac{\partial \mathbf{F}}{\partial z} = K\mathbf{F} \tag{A.2}$$

where

$$K = \begin{pmatrix} 0 & 0 & -\frac{1}{\omega}\frac{\partial}{\partial x}\left(\frac{1}{\varepsilon}\frac{\partial}{\partial y}\right) & \omega\mu + \frac{1}{\omega}\frac{\partial}{\partial x}\left(\frac{1}{\varepsilon}\frac{\partial}{\partial x}\right) \\ 0 & 0 & -\omega\mu - \frac{1}{\omega}\frac{\partial}{\partial y}\left(\frac{1}{\varepsilon}\frac{\partial}{\partial y}\right) & \frac{1}{\omega}\frac{\partial}{\partial y}\left(\frac{1}{\varepsilon}\frac{\partial}{\partial x}\right) \\ \frac{1}{\omega}\frac{\partial}{\partial x}\left(\frac{1}{\mu}\frac{\partial}{\partial y}\right) & -\omega\varepsilon - \frac{1}{\omega}\frac{\partial}{\partial x}\left(\frac{1}{\mu}\frac{\partial}{\partial x}\right) & 0 & 0 \\ \omega\varepsilon + \frac{1}{\omega}\frac{\partial}{\partial y}\left(\frac{1}{\mu}\frac{\partial}{\partial y}\right) & -\frac{1}{\omega}\frac{\partial}{\partial y}\left(\frac{1}{\mu}\frac{\partial}{\partial x}\right) & 0 & 0 \end{pmatrix}. \tag{A.3}$$

Once $\mathbf{F}$ is determined, E_z and H_z are obtained from the equations

$$\frac{\partial H_y}{\partial x} - \frac{\partial H_x}{\partial y} = -\mathrm{i}\omega\varepsilon E_z \tag{A.4}$$

$$\frac{\partial E_y}{\partial x} - \frac{\partial E_x}{\partial y} = \mathrm{i}\omega\mu H_z. \tag{A.5}$$

A finite-difference version of these equations is shown in [27]. It is obvious that matrix operator K satisfies the property $K(x, y, z) = -K(x, y, -z)$, if $\varepsilon(x, y, z) = -\varepsilon(x, y, -z)$ and $\mu(x, y, z) = -\mu(x, y, -z)$ are given, and the regions with $z > 0$ and $z < 0$ are complementary media to each other.

Appendix B

When a 2×2 matrix K has a form of

$$K = \begin{pmatrix} 0 & a \\ b & 0 \end{pmatrix}, \tag{B.1}$$

an elementary calculation shows

$$\exp(\mathrm{i}Kz) = \begin{pmatrix} \cos(kz) & (\mathrm{i}/v)\sin(kz) \\ \mathrm{i}v\sin(kz) & \cos(kz) \end{pmatrix} \tag{B.2}$$

for $ab > 0$, where $k = \sqrt{ab}$ and $v = \sqrt{ab}/a$, and

$$\exp(\mathrm{i}Kz) = \begin{pmatrix} \cosh(\lambda z) & (\mathrm{i}/v)\sinh(\lambda z) \\ -\mathrm{i}v\sinh(\lambda z) & \cosh(\lambda z) \end{pmatrix} \tag{B.3}$$

for $ab < 0$, where $\lambda = \sqrt{-ab}$ and $v = \sqrt{-ab}/a$. The conditions for $\exp(\mathrm{i}Kz) = \exp(\mathrm{i}K_\mathrm{c}z_\mathrm{c})$ are $v = -v_\mathrm{c}$ and $kz = -k_\mathrm{c}z_\mathrm{c}$ for propagating waves, and $\lambda z = -\lambda_\mathrm{c}z_\mathrm{c}$ for evanescent waves. These conditions correspond to the conservations of velocity and phase, respectively.

When $a = m_\perp/\hbar$ and $b = (2/\hbar)[E - V - \hbar^2q^2/(2m_\parallel)]$, the phase conservation for any q leads to

$$\frac{z_\mathrm{c}}{z} = -\sqrt{\frac{m_\perp}{m_{\mathrm{c}\perp}}\frac{m_{\mathrm{c}\parallel}}{m_\parallel}} \tag{B.4}$$

and

$$E = \frac{Vm_\parallel - V_\mathrm{c}m_{\mathrm{c}\parallel}}{m_\parallel - m_{\mathrm{c}\parallel}}. \tag{B.5}$$

When these conditions are satisfied,

$$\frac{v'}{v} = -\sqrt{\frac{m_\perp m_\parallel}{m_{\mathrm{c}\perp}m_{\mathrm{c}\parallel}}} \tag{B.6}$$

for $m_\perp m_{\mathrm{c}\perp} < 0$. Therefore the velocity conservation leads to

$$m_\perp m_\parallel = m_{\mathrm{c}\perp}m_{\mathrm{c}\parallel}. \tag{B.7}$$

Appendix C

The effective-mass equation shown in equation (35) is written as [19]

$$\begin{pmatrix} 0 & \mathrm{e}^{-\mathrm{i}\theta}\gamma(-\mathrm{i}\hat{k}_{x'} + \hat{k}_{y'}) & 0 & 0 \\ \mathrm{e}^{\mathrm{i}\theta}\gamma(\mathrm{i}\hat{k}_{x'} + \hat{k}_{y'}) & 0 & 0 & 0 \\ 0 & 0 & 0 & \mathrm{e}^{\mathrm{i}\theta}\gamma(-\mathrm{i}\hat{k}_{x'} - \hat{k}_{y'}) \\ 0 & 0 & \mathrm{e}^{-\mathrm{i}\theta}\gamma(\mathrm{i}\hat{k}_{x'} - \hat{k}_{y'}) & 0 \end{pmatrix} \times \begin{pmatrix} F_\mathrm{A}^\mathrm{K} \\ F_\mathrm{B}^\mathrm{K} \\ F_\mathrm{A}^{\mathrm{K}'} \\ F_\mathrm{B}^{\mathrm{K}'} \end{pmatrix} = E \begin{pmatrix} F_\mathrm{A}^\mathrm{K} \\ F_\mathrm{B}^\mathrm{K} \\ F_\mathrm{A}^{\mathrm{K}'} \\ F_\mathrm{B}^{\mathrm{K}'} \end{pmatrix} \tag{C.1}$$

where the x' and y' axes are shown in figure 3. θ is the angle between the xy and $x'y'$ axes. The equation above is obtained from $\mathrm{i}\hat{k}_x \pm \hat{k}_y = \mathrm{e}^{\pm\mathrm{i}\theta}(\mathrm{i}\hat{k}_{x'} \pm \hat{k}_{y'})$. This result shows that the rotation of the system is equivalent to the change in the relative phase between envelope functions. If we assume a plane wave with wavenumber $k_{y'}$ for the y' direction, the effective-mass equation is written as

$$\frac{\mathrm{d}}{\mathrm{d}x'}\begin{pmatrix} F_{\mathrm{A}}^{\mathrm{K}} \\ F_{\mathrm{B}}^{\mathrm{K}} \\ F_{\mathrm{A}}^{\mathrm{K}'} \\ F_{\mathrm{B}}^{\mathrm{K}'} \end{pmatrix} = \begin{pmatrix} -k_{y'} & \mathrm{e}^{-\mathrm{i}\theta}E/\gamma & 0 & 0 \\ -\mathrm{e}^{\mathrm{i}\theta}E/\gamma & k_{y'} & 0 & 0 \\ 0 & 0 & k_{y'} & \mathrm{e}^{\mathrm{i}\theta}E/\gamma \\ 0 & 0 & -\mathrm{e}^{-\mathrm{i}\theta}E/\gamma & -k_{y'} \end{pmatrix} \begin{pmatrix} F_{\mathrm{A}}^{\mathrm{K}} \\ F_{\mathrm{B}}^{\mathrm{K}} \\ F_{\mathrm{A}}^{\mathrm{K}'} \\ F_{\mathrm{B}}^{\mathrm{K}'} \end{pmatrix}. \tag{C.2}$$

It is clear that there are only two transformations that change the sign of the coefficient matrix in the right-hand side of the equation. One is the interchange of the A and B sublattices of two-dimensional graphite with $\theta = 0$ and the other is the interchange of the waves at K and K′ with $\theta = \pi/2$.

Appendix D

The tight-binding equations for the structure shown in figure 4(a) are given by

$$Ea_n = -b_n - b_{n-1} - \mu b_{n-1} \tag{D.1}$$

and

$$Eb_n = -a_n - a_{n+1} - \frac{1}{\mu}a_{n+1} \tag{D.2}$$

where $\mu = \mathrm{e}^{\mathrm{i}k}$ with wavenumber k parallel to the interface. The energy E and wavenumber k are expressed in the units of the transfer energy and the inverse of the lattice constant, respectively. The solution of these equations for $E = 0$ is given by

$$a_{n+1} = -\frac{\mu}{1+\mu}a_n \tag{D.3}$$

with $b_n = 0$ or

$$b_{n+1} = -(1+\mu)b_n \tag{D.4}$$

with $a_n = 0$. When $|k| < 2\pi/3$, the former and latter solutions are growing and decaying waves, respectively. The growing and decaying waves interchange in the other regions of the Brillouin zone.

The tight-binding equations at the interface give

$$a'_0 = b_0 \tag{D.5}$$

and

$$b'_0 = -a_0. \tag{D.6}$$

This means that all decaying waves are changed to growing waves and vice versa in the full range of the Brillouin zone. Note that the amplitude at the site symmetrical about the interface line to the site with amplitude a_{-n} is not b'_n but $\mu^{-n}b'_n$. Therefore the complementary condition including the information of phase is satisfied in the full range of the Brillouin zone for each sublattice. The only deviation from the complete complementary system is the change in the relative phase between the A and B sublattices by π in passing through the interface. The difference in phase by π is compensated in passing through another interface. Therefore a completely complementary system is formed by inserting two parallel interfaces into a graphitic lattice.

Appendix E

The tight-binding equations for the structure shown in figure 4(b) are given by

$$Ea_n = -b_n - b_{n-1} - \frac{1}{\mu}b_{n+1} \tag{E.1}$$

and

$$Eb_n = -a_n - \mu a_{n-1} - a_{n+1} \tag{E.2}$$

where μ and E are the same as those in appendix D. It is convenient to express these tight-binding equations in terms of $\tilde{a}_n$ and $\tilde{b}_n$ defined by $a_n = \mu^{\frac{n}{2}}\tilde{a}_n$ and $b_n = \mu^{\frac{n}{2}}\tilde{b}_n$. The tight-binding equations become symmetrical about the interchange of $\tilde{a}_{n+1}$ ($\tilde{b}_{n+1}$) and $\tilde{a}_{n-1}$ ($\tilde{b}_{n-1}$).

The tight-binding equations at the interface give interface matrices for $E = 0$ as

$$\begin{pmatrix} \tilde{a}'_1 \\ \tilde{a}'_0 \end{pmatrix} = \begin{pmatrix} 0 & 1 \\ 1 & 0 \end{pmatrix} \begin{pmatrix} \tilde{a}_0 \\ \tilde{a}_{-1} \end{pmatrix} \tag{E.3}$$

and

$$\begin{pmatrix} \tilde{b}'_1 \\ \tilde{b}'_0 \end{pmatrix} = \begin{pmatrix} 0 & -1 \\ -1 & 0 \end{pmatrix} \begin{pmatrix} \tilde{b}_0 \\ \tilde{b}_{-1} \end{pmatrix}. \tag{E.4}$$

These equations and the symmetrical property of the tight-binding equations in equations (E.1) and (E.2) lead to $\tilde{a}'_n = \tilde{a}_{-n}$ and $\tilde{b}'_n = -\tilde{b}_{-n}$. Since the amplitude at the site symmetrical about the interface line to the site with amplitude a_{-n} is $\mu^{-n}a'_n$, the complementary condition including the information of phase is satisfied in the full range of the Brillouin zone for each sublattice. In this case also the incompleteness in the conditions for complementary systems is only the change in the relative phase between the A and B sublattices, and a complementary system is formed by introducing double interfaces into a graphitic lattice.

References

[1] Pendry J B and Ramakrishna S A 2003 *J. Phys.: Condens. Matter* **15** 6345
[2] Veselago V G 1968 *Sov. Phys.—Usp.* **10** 509
[3] Pendry J B 2000 *Phys. Rev. Lett.* **85** 3966
[4] A recent review: Ramakrishna S A 2005 *Rep. Prog. Phys.* **68** 449
[5] Ruppin R 2004 *J. Phys.: Condens. Matter* **16** 8807
[6] A recent review: Pong W and Durkan C 2005 *J. Phys. D: Appl. Phys.* **38** R329
[7] Feenstra R M, Woodall J M and Pettit G D 1993 *Phys. Rev. Lett.* **71** 1176
[8] Johnson M B, Albrektsen O, Feenstra R M and Salemink H W M 1993 *Appl. Phys. Lett.* **63** 2923
[9] Zheng J F, Liu X, Newman N, Weber E R, Ogletree D F and Salmeron M 1994 *Phys. Rev. Lett.* **72** 1490
[10] van der Wielen M C M M, van Roij A J A and van Kempen H 1996 *Phys. Rev. Lett.* **76** 1075
[11] A comprehensive review: Ebert Ph 1999 *Surf. Sci. Rep.* **33** 121
[12] Kobayashi K 1996 *Phys. Rev.* B **53** 11091
[13] Kobayashi K 1996 *Phys. Rev.* B **54** 17029
[14] Tersoff J and Hamann D R 1985 *Phys. Rev.* B **31** 805
[15] Ando T and Mori S 1982 *Surf. Sci.* **113** 124
[16] Ando T, Wakahara T and Akera H 1989 *Phys. Rev.* B **40** 11609
[17] Zhang Y, Flugel B and Mascarenhas A 2003 *Phys. Rev. Lett.* **91** 157404
[18] For example, Painter G S and Ellis D E 1970 *Phys. Rev.* B **1** 4747
[19] Ajiki H and Ando T 1993 *J. Phys. Soc. Japan* **62** 1255
[20] Matsumura H and Ando T 1998 *J. Phys. Soc. Japan* **67** 3542
[21] Dresselhaus M S, Dresselhaus G and Saito R 1992 *Phys. Rev.* B **45** 6234
[22] Charlier J C, Gonze X and Michenaud J P 1991 *Phys. Rev.* B **43** 4579
[23] Koutecký J and Tomášek M 1960 *Phys. Rev.* **120** 1212
[24] Kobayashi K 1993 *Phys. Rev.* B **48** 1757
[25] Fujita M, Wakabayashi K, Nakada K and Kusakabe K 1996 *J. Phys. Soc. Japan* **65** 1920
[26] Kobayashi K 2005 *Surf. Sci.* **583** 16
[27] Pendry J B 1996 *J. Phys.: Condens. Matter* **8** 1085